

## Mineralogy and Genesis of Bentonites from the Tertiary Formations in Geumgwangdong Area, Korea

Soo Jin Kim\*, Jin Hwan Noh\*\* and Jae Young Yu\*

**Abstract:** Bentonites from the Janggi Group of the Lower Miocene age from the Geumgwangdong area, Korea, have been studied for mineralogical and genetic characterization. The Janggi Group is subdivided, in ascending order, into the Janggi Conglomerate, the Nuldaeri Tuff, the Geumgwangdong Shale, the Lower Coal-bearing Formation, the Basaltic Tuff, and the Upper Coal-bearing Formation. Bentonites occur as thin or thick beds in all sedimentary units of the Janggi Group, except for the Janggi Conglomerate. Significant bentonite deposits are found in the Nuldaeri Tuff, the Lower Coal-bearing Formation and the Basaltic Tuff.

Bentonites consist mainly of smectite (mainly montmorillonite), with minor quartz, cristobalite, opal-CT and feldspar. Occasionally, kaolinite, clinoptilolite or gypsum is associated with bentonites. Bentonites were studied by the methods of petrographic microscopy, X-ray diffraction, thermal analysis (DTA and TG), infrared absorption spectroscopic analysis, SEM, intercalation reaction, and chemical analysis.

Smectites commonly occur as irregular boxwork-like masses with characteristic curled thin edges, but occasionally as smoothly curved to nearly flat thin flakes. Most of smectites have layer charge of 0.25~0.42, indicating typical montmorillonite. Crystal-chemical relations suggest that Fe is the dominant substituent for Al in the octahedral layer and there are generally no significant substituents for Si in the tetrahedral layer. Ca is the dominant interlayer cation in montmorillonite. Therefore, montmorillonite from the study area is dioctahedral Ca-montmorillonite.

Occurrence and fabrics of bentonites suggest that smectites as well as cristobalite, opal-CT and zeolites have been formed diagenetically from tuffaceous materials. The precursor of smectites is trachytic or basaltic tuff. Smectites derived from the former contain relatively more  $Al_2O_3$  and less  $Fe_2O_3$  than those from the latter.

### INTRODUCTION

Occurrence of bentonites is widely reported from the Tertiary sedimentary formations of the Janggi Group in the Yeongil area. Montmorillonite is the major constituent clay mineral of bentonites and acid clays.

Bentonites from the area have been studied by Kim and Moon (1980, 1982) and Noh et al. (1983). Zeolites from the area have been studied

by Sang (1976), Kim et al. (1978, 1980, 1981), Noh and Kim (1982), and Kim et al. (1983). Recent studies by Noh and Kim (1982), Kim et al. (1983) and Noh (1985) show that the zeolites as well as smectites from the area have been formed by diagenetic processes from the tuffs in the non-marine environment.

### GENERAL GEOLOGY

Geology of the area consists of rhyolites of Mesozoic age, the sedimentary rocks of the Janggi Group of Lower Miocene age, and volcanic rocks of Quaternary age. The Janggi Group

\* Department of Geological Sciences,  
Seoul National University

\*\* Department of Geology,  
Kangweon National University

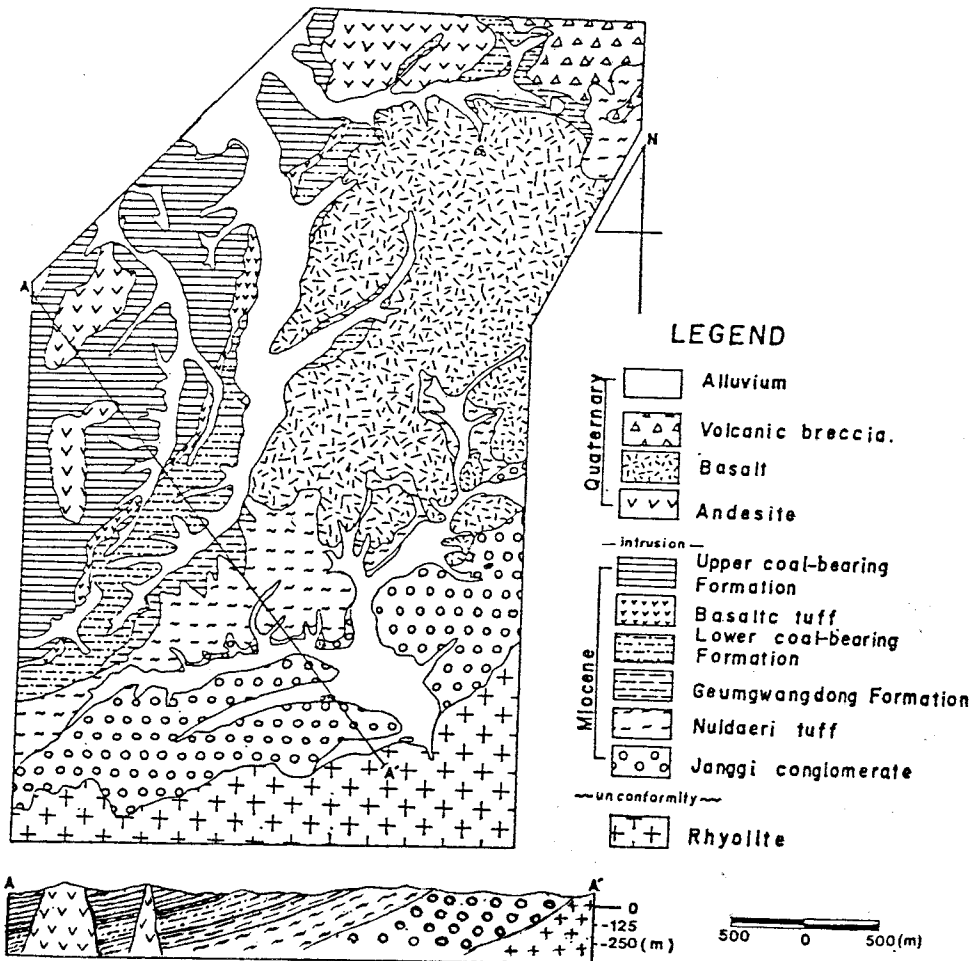


Fig. 1 Geological map and cross section of the Geumgwangdong area.

is intruded or overlain by andesite, basalt and basaltic volcanic breccia (Fig. 1).

The Janggi Group is subdivided, in ascending order, into the Janggi Conglomerate, the Nuldaeri Tuff, the Geumgwangdong Formation, the Lower Coal-bearing Formation, the Basaltic Tuff and the Upper Coal-bearing Formation. Detailed stratigraphic sequence is shown in Fig. 2. The general attitude of the Janggi Group is N45°E in strike and 20°NW in dip.

**OCCURRENCE OF BENTONITES**

Bentonites occur as continuous or discontinuous thin or thick beds in every rock unit except the Janggi Conglomerate of the Janggi Group.

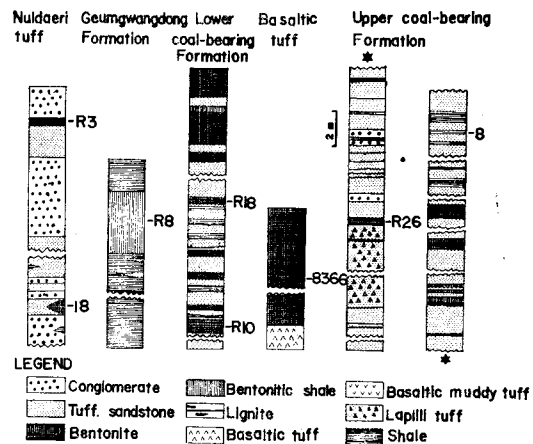


Fig. 2 Stratigraphic columns of the Janggi Group showing the intercalation of bentonite beds.

But, the economic reserves are mainly found in the Nuldaeri tuff, the Lower Coal-bearing Formation, the Basaltic Tuff, and the Upper Coal-bearing Formation. Nearly all the tuffaceous materials in the area are more or less smectitized.

In the Nuldaeri tuff, bentonite is found in the fine-grained tuff, but also in the lapilli tuff. It is often found that fragments and matrices of lapilli tuff are all together bentonitized. Tuffaceous materials in sandstones are also bentonitized. In the Geumgwangdong Formation, shale is deeply smectitized. In the Lower Coal-bearing Formation and the Upper Coal-bearing Formation, bentonite is found as thick or thin beds alternating with lignite and sandstone. In the Basaltic Tuff, the basaltic materials are transformed to the greenish bentonites.

Bentonites show grey, green, dark green, pink, or yellow color in the field. Grey or dark green color of bentonites is due to the presence of carbonaceous materials, whereas yellow, brown, or green color is due to the presence of iron.

## EXPERIMENTS

### Materials

Samples were collected from the important

bentonite horizons of the Janggi Group in the Geumgwangdong area. Sample numbers are shown in the columnar sections in Fig. 2.

### Preparation of samples

The about 2  $\mu\text{m}$  clay fractions were separated by sedimentation and centrifugation with distilled water for various experiments. Organic matter was removed with  $\text{H}_2\text{O}_2$ . Thin sections were also prepared for the study of fabrics of bentonites and associated rocks.

### Methods

The mineralogical analysis (Table 1) of all the untreated as well as treated samples were carried out by powder X-ray diffraction (XRD) using a JEOL X-ray diffractometer with  $\text{CuK}\alpha$  radiation. Basal spacing,  $d_{(001)}$  was measured on oriented samples. The oriented samples were further examined by XRD after intercalation with ethylene glycol and n-alkylammonium.

Differential thermal analysis (DTA) and thermogravimetric analysis (TG) were carried out with a Du Point thermal analyzer on about 50 mg of powder sample at a heating rate of  $10^\circ\text{C}/\text{min}$  in air.

Infrared absorption spectra in the range of  $200\sim 4000\text{ cm}^{-1}$  were obtained with a Perkin-

Table 1 Mineral composition of bentonites of each formation in Geumgwangdong area.

sample number	color	mineral composition							remarks
		M	K	Q	Cr	F	O	C	
8	brownish white	###		+	+	+	+		Upper Coal-bearing Formation
R 26	dark green	###		+	+	+	+		
8368	green	###		+	+	+			
8367	green	###		+	+	+	+	+	Basaltic tuff
8366	green	###		+	+	+	+	+	
R 18	yellow	###	+	+	+	+	+		Lower Coal-bearing Formation
R 14	dark green	###	+	##	+	+	+		
R 8	brown	###	+	+		+	##		Geumgwangdong F.
R 3	dark green	###		+	+	+	+	+	Nuldaeri tuff
19	pink	###		+	+	+	##		

M : montmorillonite, K : kaolinite, Q : quartz, Cr : cristobalite, F : feldspar, O : opal-CT, C : clinoptilolite.  
### : very much, ## : medium, + : small, + : very small

**Table 2** Chemical composition of bentonites and associated rocks from Geumgwangdong area (sample numbers as in Table 1).

	6	R26	8368	8367	8366	R18	R14	R10	4	R3
SiO <sub>2</sub>	64.80	52.56	56.84	54.24	53.96	51.14	55.48	57.30	62.22	57.67
TiO <sub>2</sub>	0.28	0.80	0.96	1.03	1.16	0.72	0.74	0.59	0.39	0.60
MnO <sub>2</sub>	0.09	0.06	0.05	0.09	0.07	0.12	0.04	0.06	0.08	0.06
Al <sub>2</sub> O <sub>3</sub>	14.18	16.81	17.63	16.60	18.42	18.45	21.02	19.23	16.31	17.43
Fe <sub>2</sub> O <sub>3</sub>	2.25	3.79	5.25	6.48	6.32	5.53	3.48	2.67	2.57	3.30
FeO	0.30	0.22	0.37	1.03	tr	tr	0.22	1.03	0.07	0.96
MgO	2.09	1.27	2.25	2.90	1.99	1.87	1.47	1.85	1.11	1.07
CaO	1.32	1.44	3.02	2.39	2.45	1.12	1.38	1.18	1.04	1.70
Na <sub>2</sub> O	2.83	1.11	2.40	0.94	1.01	0.41	1.60	1.59	1.82	1.60
K <sub>2</sub> O	2.90	0.93	0.69	0.47	0.63	0.63	1.73	1.96	2.82	1.12
Li <sub>2</sub> O	—	tr	—	—	—	—	0.01	tr	—	tr
H <sub>2</sub> O(+)	4.90	6.53	4.82	6.90	6.62	7.03	5.30	5.13	6.33	5.27
H <sub>2</sub> O(-)	2.85	13.39	3.02	5.72	6.32	12.31	5.23	6.33	4.12	9.00
Ig. loss	1.17	1.06	2.65	1.19	1.03	0.65	2.27	1.07	1.11	0.20
Total	99.96	99.97	99.95	99.98	99.98	99.98	99.97	99.99	99.99	99.98

6) White bentonite; R26) Greenish bentonite; 8368, 8367, 8366) Greenish bentonites; R18) Yellowish bentonite; R14) dark green bentonite; R10) dark green bentonite; 4) Bentonitic tuff; R3) Greenish bentonite

Elmer 283D spectrophotometer on approximately 2 mg of powder sample dispersed in potassium bromide disk.

Chemical analysis of the raw and separated samples was made by the wet method as well as X-ray fluorescence (XRF) spectrometer method. Fe<sup>2+</sup> and Fe<sup>3+</sup> were analyzed by wet method. H<sub>2</sub>O(+) and H<sub>2</sub>O(-) were determined

by thermogravimetry.

### MINERALOGY OF BENTONITES

Mineral compositions of various types of raw bentonites and associated bentonitic rocks were determined by XRD (Table 1). Although montmorillonite is the major constituent clay mineral of bentonites, a small amount of other minerals

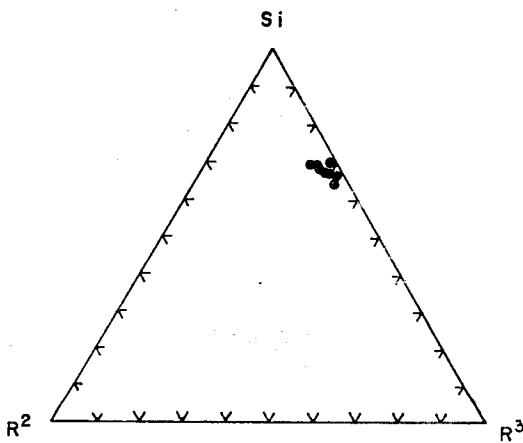


**Fig. 3** Si-R<sup>2+</sup>-R<sup>3+</sup> diagram showing the chemical variation in montmorillonites. Si=SiO<sub>2</sub>; R<sup>2+</sup>=Mg<sup>2+</sup>+Fe<sup>2+</sup>; R<sup>3+</sup>=Al<sup>3+</sup>+Fe<sup>3+</sup>+Ti<sup>4+</sup>.

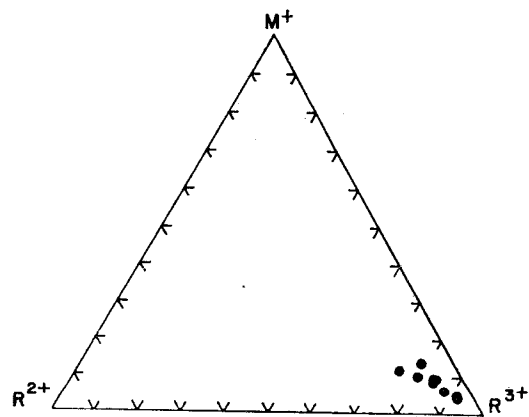
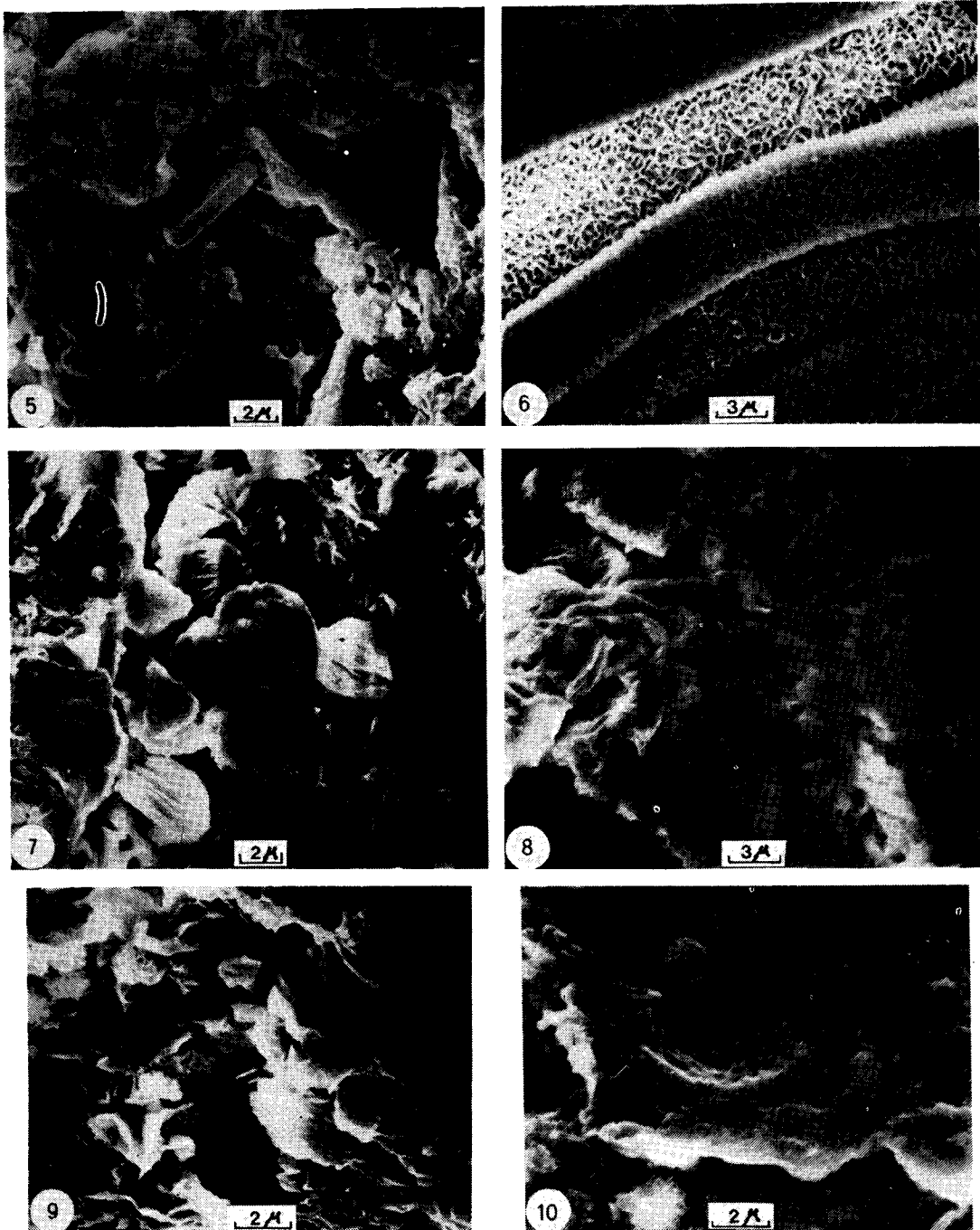
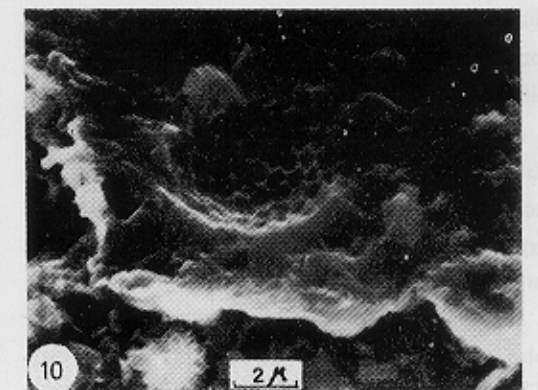
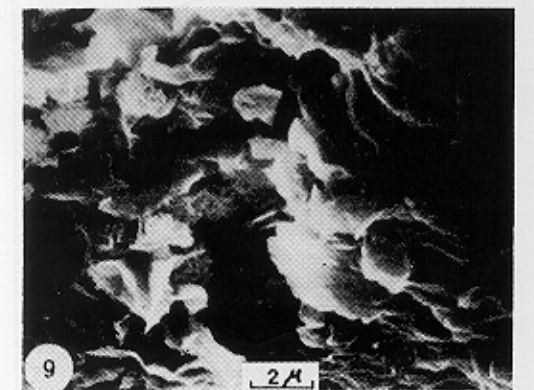
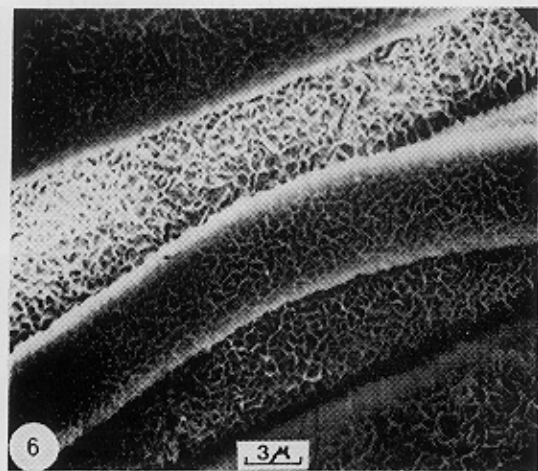
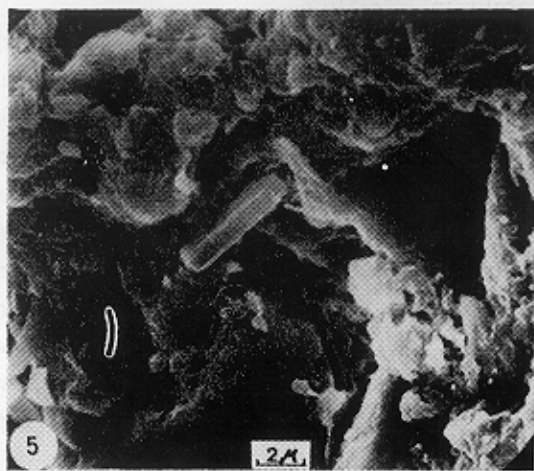


**Fig. 4** M<sup>+</sup>-R<sup>2+</sup>-R<sup>3+</sup> diagram showing the chemical variation in montmorillonites. M<sup>+</sup>=Na<sup>+</sup>+K<sup>+</sup>+2Ca<sup>2+</sup>; R<sup>2+</sup>=Mg<sup>2+</sup>+Fe<sup>2+</sup>; R<sup>3+</sup>=Al<sup>3+</sup>+Fe<sup>3+</sup>+Ti<sup>4+</sup>.



**Figs. 5~10** SEM micrographs of montmorillonites from the Geumgwangdong area.

5) Montmorillonite flakes growing at expense of volcanic glass (massive) (sample No. R10). 6) Sponze-like aggregates of montmorillonites (sample No. R26). 7) Globular aggregates of well-crystallized montmorillonite flakes in association with opal-CT lepispheres (sample No. 18). 8) Curled flakes of montmorillonites (Sample No. 8368). 9) Cristobalite growing on the montmorillonite flakes (sample No. R10). 10) Montmorillonite preserving the original structure of diatom. Note the opal-CT lepisphere at the bottom (Sample No. R8).



Figs 5-10 SEM micrographs of montmorillonites from the Gaomangdong area

such as quartz, cristobalite, feldspar, opal-CT, clinoptilolite, and kaolinite are also included.

Biotite is included in sandstone or slightly smectitized tuff. Although clinoptilolite is found as trace in most of the area, it occurs abundantly in association with mordenite in the northeastern corner of the area.

Table 2 shows the chemical composition of raw bentonites. The average  $\text{SiO}_2/\text{Al}_2\text{O}_3$  ratio is 3.54. The high  $\text{SiO}_2$  content is correlated with high content of quartz. The high content of  $\text{Al}_2\text{O}_3$  and  $\text{K}_2\text{O}$  is correlated with the content of kaolinite and K-feldspar, respectively.

Figs. 3 and 4 show the chemical distribution in bentonites.  $\text{M}^+$  is the interlayer cations including Na, K and 2Ca.  $\text{R}^{2+}$  is divalent cations including  $\text{Mn}^{2+}$  and  $\text{Fe}^{2+}$ .  $\text{R}^{3+}$  is trivalent cations including  $\text{Al}^{3+}$  and  $\text{Fe}^{3+}$  together with  $\text{Ti}^{4+}$ .

### Montmorillonite

Montmorillonite is the major constituent mineral of bentonites. It shows curled thin edges under SEM (Figs. 5~10). They generally form honey-comb-like (Fig. 6), but occasionally globular aggregates (Fig. 7) in places.

The presence of  $1.5\text{\AA}$  reflection in the XRD pattern indicates that the montmorillonites from the area is dioctahedral. The globular montmorillonite is well crystallized, showing nice X-ray diffraction pattern.

Chemical analyses show that Fe is the dominant substituent for Al in the octahedral layer, and no significant substituent exist in the tetrahedral layer except in sample R14. Ca is the dominant interlayer cation.

DTA and TG curves of montmorillonite samples are shown in Fig. 11 and 12, respectively. The endothermic peaks from  $100\sim 110^\circ\text{C}$  are due to the dehydration of interlayer water between silicate layers. Poorly defined shoulder at  $140^\circ\text{C}$  in sample R14 is probably related to the dehydration of cation-coordinated water. TG curves show that the rapid dehydration took place

between  $100\sim 250^\circ\text{C}$ .

The dehydroxylation peak temperatures vary between  $420\sim 600^\circ\text{C}$ . Most of samples except the sample 8 show dual dehydroxylation endothermic peak in the same temperature range. Dual peaks between  $420\sim 600^\circ\text{C}$  suggest that the samples are "abnormal" montmorillonite. Dual peaks have been explained as due to bimineralic mixtures (Jonas, 1955), structural irregularities (Greene-Kelly, 1957) and mixing of layers (Grim and Kulbicki 1961; Grim, 1968). Grim (1968) shows the possibility of kaolinite or halloysite as impurities.

The endothermic peak at  $420^\circ\text{C}$  in Sample 8 is due to the high content of iron (0.32 atoms per half cell). The endothermic peak at about  $600^\circ\text{C}$  is characteristic of montmorillonite having the iron content in the range  $0.19\sim 0.27$  atoms per half cell. The abrupt weight loss between  $400\sim 700^\circ\text{C}$  in TG curves is due to the dehydroxylation.

The XRD patterns of heat-treated samples at various temperatures are shown in Fig. 13. The

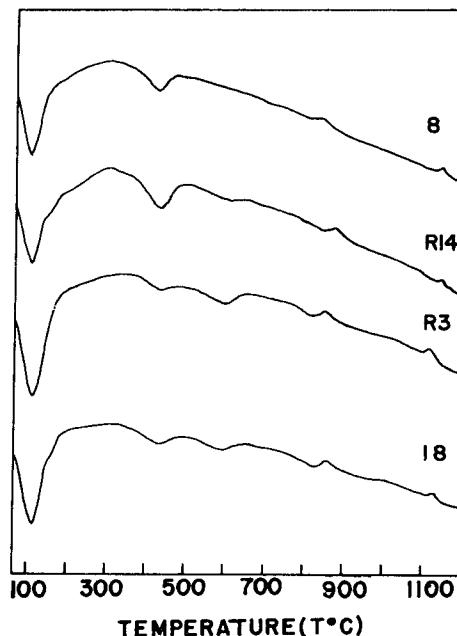


Fig. 11 DTA curves of montmorillonites from the Geumgwangdong area.

14Å, d-spacing of (001) of montmorillonite at 65°C is abruptly decreased to about 10Å at 165°C. The interlayer water is almost dehydrated at this temperature, leaving only small amount of water to be escaped up to about 375°C. Above 165°C, the (001) basal spacing is nearly constant. The 7.1Å reflection of kaolinite impurity disappears between 370~500°C.

IR spectral data indicate that the samples are typical montmorillonite species (Fig. 14). Throughout the region of 3000~4000 cm<sup>-1</sup>, they show two maxima, namely, one fairly narrow band at 3620~3640 cm<sup>-1</sup>, and another broad band at 3410~3440 cm<sup>-1</sup>, which are the characteristic vibrations of interlayer water. IR patterns of Si-O stretching and bending vibrations, and O-H bending vibration throughout the region of 400~1800 cm<sup>-1</sup> also show those of typical montmorillonite.

Montmorillonite-organic reactions have been studied for better identification and characterization of montmorillonite. Ethylene glycol, gly-

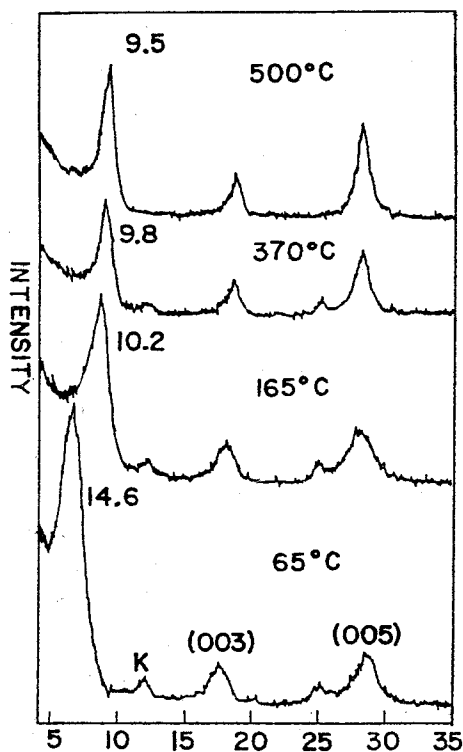


Fig. 13 XRD patterns of sample R18 at various temperatures.

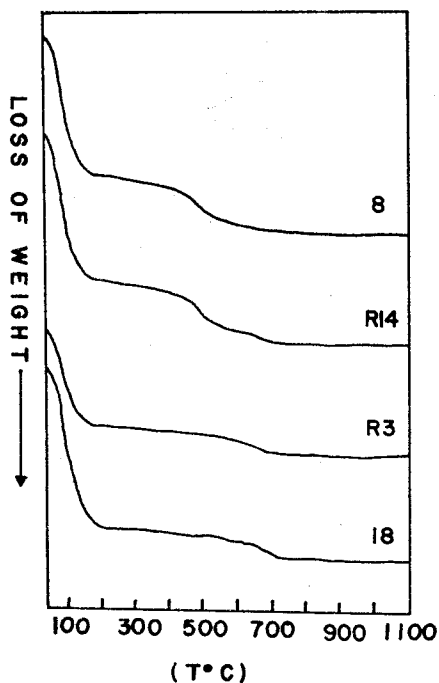


Fig. 12 TG curves of montmorillonites from the Geumwangdong area.

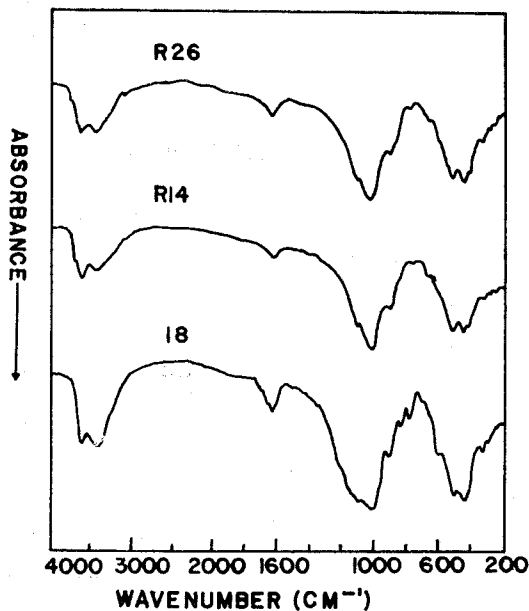


Fig. 14 IR spectra of montmorillonites from the Geumwangdong area.



cerol and *n*-alkylammonium were used for organic intercalation with montmorillonite. *n*-alkylammonium intercalation experiment was carried out by the procedure of Lagaly and Weies (1969, 1970).

Fig. 15 shows the shifting of basal reflection in montmorillonite treated with ethylene glycol and glycerol, respectively. The (001) spacing increased to about 17Å by glycolation and to 17.8Å by glycerol intercalation. Kaolinite peak has not shifted after these intercalation experiment. This result suggests that the sample R18 is a mixture of montmorillonite and kaolinite, without forming mixed-layer clay.

Fig. 16 shows shifting of basal spacings in montmorillonite by intercalation of *n*-alkylammonium ion of various chain numbers. Calculated layer charges and cation exchange capacities calculated from Fig. 16 are summarized in Table 3. From this table, it can be seen that samples

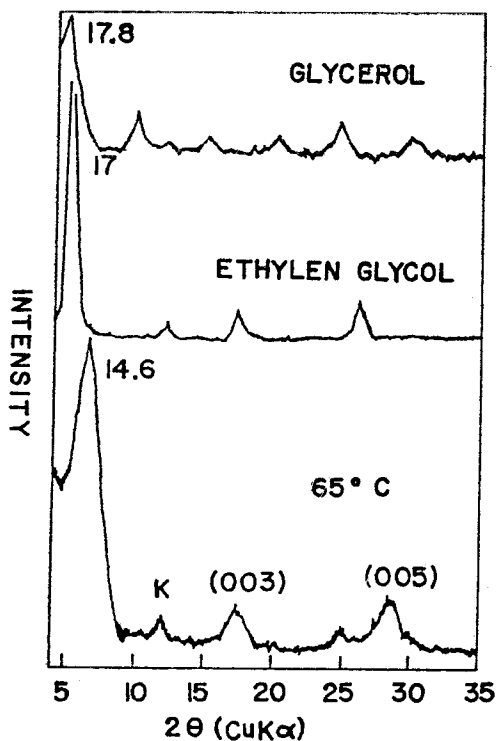


Fig. 15 Variation of  $d_{(001)}$  spacing of montmorillonites at various intercalation. K is kaolinite.

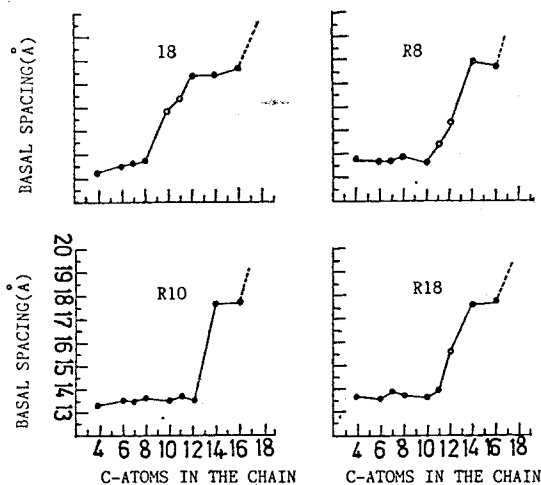


Fig. 16 Variation of basal spacings of *n*-alkylammonium derivatives of montmorillonites from the Geumwgangdong area.

have heterogeneous charge distribution of 0.25 ~ 0.42/(Si, Al)<sub>4</sub>O<sub>10</sub> and cation exchange capacity of 77~103 meq/100g. The high layer charge and CEC of sample 18 is attributed to the considerable substitution of Al by Mg in octahedral layer. The relatively high layer charge and cation exchange capacity of sample R14 are due to the considerable substitution of Al for Si in tetrahedral layer.

Table 3 Layer charge and cation exchange capacity of montmorillonites.

sample No.	limiting values of cation density Eq./ $(\text{Si, Al})_4\text{O}_{10}$	calculated cation exchange capacity meq./100g
8	0.36~0.25	80.62
R26	0.33~0.25	80.62
8366	0.31~0.25	77.84
R18	0.33~0.28	86.18
R10	0.31~0.28	80.62
R8	0.36~0.28	88.96
R3	0.36~0.25	77.84
18	0.42~0.31	101.86

#### Silica minerals

Silica minerals associated with bentonites are quartz, cristobalite and opal-CT.

Quartz is a ubiquitous accessory mineral in bentonites. It occurs as microcrystalline or cryptocrystalline aggregates. Most of quartz is detrital in origin. But some of quartz occur as precipitates in association with clinoptilolite in bentonite.

Cristobalite is a common silica mineral in bentonite. It is characterized by its sharp (101) reflection at 4.05Å. It occurs as minute spherical aggregate less than 5µm in size (Fig. 7).

Opal-CT is found in the bentonites in the Nuldaeri tuff and the bentonitic shale of the Geumgwangdong Formation. It is distinguished from other types of silica minerals by its characteristic two broad peaks at 4.13Å and 2.51Å. It usually occurs as lepispheres in the cavities in bentonites (Figs. 9 and 10). It is significant to note that opal-CT is the major constituent of the well-laminated shale of the Geumgwangdong Formation.

#### **Feldspar**

K-feldspar occurs as cryptocrystalline, subhedral to euhedral crystals in pores of bentonite (Fig. 5).

#### **Clinoptilolite**

Clinoptilolite occurs as cryptocrystalline to microcrystalline pseudomorphs after glass shards or new crystals in pores of bentonites. It shows tabular habit. Detailed descriptions of zeolites from this area (especially in the Danghae clay deposits) are found in Kim and Noh (1983).

#### **Kaolinite**

Kaolinite occurs as accessory mineral in some bentonites, sandstone, shale and lapilli tuff. It probably is the weathering product of montmorillonite. The basal spacing of kaolinite has not shifted in the organic intercalation experiment (Fig. 15). This suggests that it is included without forming mixed-layer clay with montmorillonite.

## **GENESIS OF BENTONITES**

Evidences supporting the working hypothesis for the formation of certain ore deposits should be given on every scale: on regional, local, outcrop, handspecimen, and microscopic scales. Bentonites occur as nearly uniform, thick or thin beds in the sedimentary formations of the Janggi Group. Bentonite beds are alternated with lignite and sandstone. Such stratigraphic sequence is found not only on the local scale, but also on the regional scale. The congruent relationship of the bentonite beds to the overlying and the underlying beds is one of the strong evidences for the syngenetic deposition. But this does not always mean that the bentonite materials precipitated as mineral smectite. It is important to note that nearly all the rocks of the Janggi Group are more or less smectitized.

On the outcrop or handspecimen scale, smectite-bearing rocks including bentonites show well-developed stratification. Lapilli or ash tuff is also smectitized without destruction of the rock fabrics. Tuff fragments and matrices are all together smectitized. A close association of bentonite with lignite beds suggests that bentonite was formed in the swamp or shallow lacustrine environment. On the microscopic scale, the following phenomena are observed.

- 1) Glass shards are replaced by montmorillonite pseudomorphously.
- 2) Montmorillonite aggregates show honeycomb fabric, indicating the crystallization from solution.
- 3) Diatoms are pseudomorphously replaced by montmorillonite preserving the original organic structure.
- 4) Cristobalite and opal-CT are crystallized in pores within the montmorillonite aggregates.
- 5) Montmorillonite is replaced by clinoptilolite.
- 6) Clinoptilolite is also crystallized in pores within bentonite.

Based on above observations of various scales, the process of formation of bentonite in the Tertiary formations. is suggested as in the following.

The first stage of the formation of bentonite is the deposition of tuffaceous materials in the swamp or shallow lacustrine environment. Especially the deposition of volcanic glass is prerequisite. The second stage is the reaction of volcanic glass with pore solution. This reaction resulted in the partial dissolution of glass and the formation of montmorillonite in the pseudomorphous or fractional way. Occurrence of montmorillonite supports this. The formation of montmorillonite was probably favored by a relatively low  $(\text{Na}^+ + \text{K}^+)/\text{H}^+$  activity ratio (Hemley, 1962) at the early stage of interaction of volcanic glass with pore solution. Extensive and widespread occurrence of montmorillonite in the Tertiary formations suggests that the concentration of alkali ions remained low for a long time for the continued formation of montmorillonite in the basin. Localization of zeolite occurrence in certain horizons suggest that the pH and the concentration of alkali ions in the pore solution have increased at certain stage, providing a chemical environment more favorable for the formation of clinoptilolite rather than montmorillonite. Barrows (1980) shows that the favorable conditions for the formation of clinoptilolite are high Si/Al and alkali ions/H ion activity ratios. Cristobalite and opal-CT were formed from the excess silica in pore solution which was produced by crystallization of montmorillonite. Some of silica was probably supplied by biogenic organism.

### SUMMARY AND CONCLUSIONS

Results of study on the mineralogy and genesis of bentonite from the Geumgwangdong area are summarized in the following.

1) Significant bentonite deposits are found

in the Nuldaeri Tuff, the Lower Coal-bearing Formation and the Basaltic Tuff.

2) Bentonites consist mainly of montmorillonite with minor quartz, cristobalite, opal-CT and feldspar. Occasionally, kaolinite, clinoptilolite or gypsum is associated with bentonites.

3) Montmorillonites occur as irregular boxwork-like masses with characteristic curled thin edges but occasionally as smoothly curved to nearly flat thin flakes.

4) Smectites have layer charge of 0.25~0.42, indicating typical montmorillonite and cation exchange capacity of 77~89 meq/100g except the sample 18 having 102 meq/100g.

5) Crystal chemical relations suggest that Fe is the dominant substituent for Al in the octahedral layer and there are no significant substituents for Si in the tetrahedral layer. Ca is the dominant interlayer cation in montmorillonite. Therefore, smectite from the area is dioctahedral Ca-montmorillonite.

6) The dehydroxylation peak temperature of montmorillonites are relatively considerably low ranging from 400 to 600°C.

7) Occurrence and fabrics of bentonites suggest that montmorillonite as well as cristobalite, opal-CT and zeolites have been formed diagenetically from tuffaceous materials. Montmorillonite derived from the trachytic tuff contain relatively higher  $\text{Al}_2\text{O}_3$  and lower  $\text{Fe}_2\text{O}_3$  than those from the basaltic tuff.

### ACKNOWLEDGMENT

The present studies were supported by the Basic Science Research Institute Program of the Ministry of Education, 1984. Sincere thanks are extended to the Ministry of Education for the financial support.

### REFERENCES

- Barrows, K.J. (1980) Zeolitization of Miocene volcaniclastic rocks, Southern Desatoya Mountains, Nevada. *Geo. Soc. Amer. Bull.* Part 1. No.91, p.199-

- 201.
- Green-Kelly, R. (1957) The differential thermal analysis of clays, Mineralogical Society, London p. 140-164.
- Grim, R.E. (1968) Clay mineralogy. McGraw-Hill.
- Grim, R.E. and Kulbicki, G. (1961) Am. Mineral., v. 46, p. 1329.
- Hemley, J. (1962) Alteration studies in the system  $\text{Na}_2\text{O}-\text{Al}_2\text{O}_3-\text{SiO}_2-\text{H}_2\text{O}$ . Geol. Soc. Amer. Spec. Paper, v. 68, p. 1-196.
- Jonas, E.C. (1955) Natl. Acad. Sci. Publ. No. 395, 66.
- Kim, J.H. and Moon, H.S. (1978) Occurrence in the Tertiary sediments. J. Korean Inst. Mining Geol., v. 11, p. 59-68.
- Kim, J.H. and Moon, H.S. (1980) Zeolites, bentonites and Fuller's earth deposits in the Tertiary sediments of Guryongpo and Gampo areas. Report on Geosci. Miner. Res., v. 8, p. 99~147.
- Kim, J.H. and Moon, H.S. (1982) Zeolite, bentonite and Fuller's earth deposits in Tertiary sediments, Yeongil and Gampo areas. Report on Geosci. Miner. Res., v. 10, p. 105-124.
- Kim, S.J., Sang, K.N., and Noh, J.H. (1983) Mineralogy and genesis of zeolites in Tertiary formations in Yeongil area. J. Geol. Soc. Korea, v. 19, p. 227-236.
- Lagaly, G. and Weiss, A. (1969) Determination of the layer charge in mica type layer silicates. Proc. Intern. Clay Conf., Tokyo, v. 1, p. 66-88.
- Lagaly, G. and Weiss, A. (1970) Reunion Hispano-Belga de Minerals de la Arcilla, Madrid, 179.
- Noh, J.H. and Kim, S.J. (1982) Mineralogy and genesis of zeolites from the Tertiary tuffaceous rocks in Guryongpo area. J. Geol. Soc. Korea, v. 18, p. 1-10.
- Noh, J.H., Kim S.J. and Choy, J.H. (1983) Mineralogical and chemical characterization of bentonites from Tertiary tuffaceous sediments in the Donghae Bentonite Mine. J. Geol. Soc. Korea, v. 19, p. 39-48.
- Noh, J.H. (1985) Mineralogy and genesis of zeolites and smectites from Tertiary tuffaceous rocks in Yeongil Area. Ph.D. thesis, Seoul National University.
- Sang, K.N. (1976) Natural zeolites. J. Korean Inst. Mining Geol., v. 9, p. 239-247.
- Sudo, T. and Shimoda, S. (1978) Clay and clay minerals of Japan. 326 pp. Elsevier Pub. Co.
- Tateiwa, (1924) Geological maps and explanation text of Yeongil and Joyang sheets. Geological map of Korea, No. 2.

### 第3紀層에賦存하는粘土鑛物에對한鑛物學的및成因的研究

金洙鎭\*·魯振煥\*\*·俞在英\*

요약 : 金光洞地域의 第3紀 下部 마이오세의 長鬚層群中에서 産出되는 벤토나이트의 鑛物學的 및 成因의 特性에 關하여 研究되었다. 벤토나이트는 長鬚礫岩을 除外한 모든 長鬚層群의 構成멤버層에서 産出된다. 그러나 重要한 벤토나이트鑛床은 主로 訥臺里凝灰岩層, 下部含炭層 및 玄武岩質凝灰岩에 賦存되어 있다.

벤토나이트는 主로 스멕타이트(主로 몬모릴로나이트)와 그리고 少量의 石英, 크리스토파라이트, 蛋白石, 長石 등으로 構成되어 있고 곳에 따라 클리놀릴로라이트, 할로이사이트, 石膏가 隨伴된다. 벤토나이트에 對하여 顯微鏡觀察, X線廻折分析, 熱分析, 赤外線分光分析, 走査電子 顯微鏡觀察, 層間化合反應, 및 化學分析 等の 方法으로 研究되었다. 스멕타이트는 보통 特徵의인 꾸부러진 緣邊部를 갖는 不規則한 스펀지 모양으로 産出되지만 境遇에 따라서는 完만하게 彎曲되거나 또는 平坦한 얇은 葉狀으로 産出되기도 한다. 대부분의 스멕타이트는 格子層間電荷가 0.25~0.42로서 典型的인 몬모릴로나이트를 指示해준다. 그러나 간혹 바이델라이트에 該當하는 格子間電荷를 보여 주는 試料도 있다. 結晶化學的 資料로 볼때 8面體構造層에서는  $\text{Fe}^{3+}$ 가  $\text{Al}^{3+}$ 을 置換하고 있으며 4面體構造層에서는  $\text{Si}^{4+}$ 가 다른 이온에 依하여 別로 置換되어 있지 않다. 層狀格子間에는 主로  $\text{Ca}^{2+}$ 가 存在한다. 따라서 이

\* 서울大學校 自然科學大學 地質科學科

\*\* 江原大學校 自然科學大學 地質學科

地域의 스멕타이트는 dioctahedral 칼슘몬모릴로나이트이다.

벤토나이트의 産出狀態와 組織은 스멕타이트, 크리스토팔라이트 蛋白石 및 沸石이 凝灰質 物質로부터 續成作用에 依하여 生成되었음을 指示하여 준다. 스멕타이트의 原岩은 粗面岩質 또는 玄武岩質 凝灰岩이며 粗面岩質凝灰岩으로 으로부터 由來된 스멕타이트는 玄武岩質 凝灰岩으로 由來된 것 보다  $Al_2O_3$ 를 높게 그리고  $Fe_2O_3$ 를 낮게 含有하고 있다.